

PVP2023-105307

UNCERTAINTIES IN IN-STRUCTURE RESPONSE SPECTRA DUE TO UNCERTAINTIES IN INPUT MOTION AMPLITUDE AND PHASE SPECTRA

Jinsuo R. Nie, Jim Xu, Vladimir Graizer, and Dogan Seber

Division of Engineering
Office of Nuclear Regulatory Research
U.S. Nuclear Regulatory Commission
Washington, DC, USA

ABSTRACT

We concluded in PVP2020-21132 that the four or five time histories in the current practice are not sufficient for estimating stable mean in-structure response spectra (ISRS), therefore a check of their power spectral density functions is necessary. The time histories used in that work were not developed based on typical response spectrum (RS) convergence criteria and did not consider the uncertainties in Fourier amplitude spectra. This paper examines how the uncertainties in both Fourier phase spectra and Fourier amplitude spectra of the input motions resulting from seed time histories and a new RS-matching algorithm affect the uncertainties in ISRS. This study finds that the coefficient of variation in ISRS reached as high as 68%, generally confirming previous results obtained using a different RS-matching algorithm. This level of ISRS variation continues to support our conclusions in PVP2020-21132. Therefore, a check of the power spectral density functions of the multiple input time histories in the current practice is necessary to ensure the estimated mean ISRS would vary on the conservative side, although not as stable as necessarily required for reasonable confidence levels. These results provide the necessary technical bases for consistent technical positions between industry standards and regulatory guide for nuclear power plants.

Keywords: confidence level; in-structure response spectrum; multiple input motions; power spectral density; wavelet based response spectrum matching

INTRODUCTION

To estimate the mean seismic responses of linear structural systems, a common practice is to use multiple response spectrum (RS)-matched input acceleration time histories in seismic analysis [1, 2]. PVP2020-21132 examined whether multiple acceleration time histories can be used to achieve stable mean responses by explicitly considering the uncertainties in the Fourier phase spectra of the input time histories while keeping their Fourier amplitude spectra constant [3]. However, constant Fourier amplitude spectra are extremely difficult, if not completely infeasible, to achieve in RS-matching algorithms. This paper examines how the uncertainties in both Fourier phase spectra and Fourier amplitude spectra of the input motions resulting from the RS-matching algorithms and seed time histories affect the uncertainties in in-structure response spectra (ISRS). We aim at generally confirming whether the coefficient of variation (COV) in ISRS, COV_{ISRS} , based on a new RS-matching algorithm is comparable to what was reported in PVP2010-25919 [4], which used a different RS-matching algorithm. A confirmed high level of COV_{ISRS} would indicate that the current practice of using the four or five time histories would not be sufficient for estimating stable mean ISRS and therefore, a check of the power spectral density (PSD) functions of these input time histories would be necessary to ensure the estimated mean ISRS would vary on the conservative side, although not as stable as necessarily required for reasonable confidence levels.

DISCLAIMER NOTICE—The findings and opinions expressed in this paper are those of the authors, and do not necessarily reflect the view of the U.S. Nuclear Regulatory Commission.

This material is declared a work of the U.S. Government and is not subject to copyright protection in the United States. Approved for public release; distribution is unlimited.

It should be noted that Section 3.7.1, “Seismic Design Parameters,” of NUREG-0800, “Standard Review Plan for the Review of Safety Analysis Reports for Nuclear Power Plants: LWR Edition” [1], already indicates the necessity of a PSD check in Option 2, “Multiple Sets of Time Histories.” This study and PVP2020-21132 can provide the quantitative reasoning for this necessity. The results in this study, PVP2010-25919, and PVP2020-21132 may provide the necessary technical bases for consistent technical positions between the American Society of Civil Engineers (ASCE)/Structural Engineering Institute (SEI) 4-16, “Seismic Analysis of Safety-Related Nuclear Structures” [2], and NUREG-0800 [1]. The current RS convergence criteria in ASCE 4-16 practically do not require a PSD check.

In our PVP2020-21132 paper [3], we demonstrated that the uncertainties in Fourier phase spectra of the input motions alone, which are considered irreducible, could result in a maximum coefficient of variation (COV) in in-structure response spectra (ISRS) (COV_{ISRS}) around 40%. With this level of COV_{ISRS} , four or five input time histories in the current practice were found not able to lead to stable ISRS estimates for reasonable confidence levels. In that paper, the Fourier amplitude spectra of the input time histories remained constant, and their uncertainties were not considered. However, we postulated that the uncertainties in Fourier amplitude spectra are expected to increase COV_{ISRS} . The input time histories in PVP2020-21132 are designated in this paper as power spectral density (PSD)-based time histories because the constant Fourier amplitude spectra were calculated from the target PSD functions described in Appendix B, “Guidance on Minimum Power Spectral Density for NUREG/CR-6728 Based Design Spectra or Other Spectra,” to Section 3.7.1, Revision 4, “Seismic Design Parameters,” issued December 2014, of NUREG-0800, “Standard Review Plan for the Review of Safety Analysis Reports for Nuclear Power Plants: LWR Edition” (SRP) [1]. On average, the response spectra of the PSD-based input time histories were essentially identical to the bin representative response spectra in the SRP.

This paper (1) assesses the uncertainties in ISRS due to uncertainties in both Fourier phase spectra and Fourier amplitude spectra of the input motions and (2) compares the results to those that only considered the uncertainties in Fourier phase spectra.

A common practice to estimate the mean seismic responses of linear structural systems is to use multiple response spectrum (RS)-matched input acceleration time histories to obtain stable estimates of the responses. The resultant time histories include uncertainties in their Fourier amplitude and phase spectra, which can be strongly influenced by the method used for RS matching. The uncertainties in the Fourier amplitude spectra of the RS-matched time histories are usually not separable from those of the Fourier phase spectra. In this paper, we use a newly developed, wavelet-based RS-matching algorithm (based on Reference [5]) to (1) explore how uncertainties in both the Fourier amplitude spectra and the Fourier phase spectra can

affect COV_{ISRS} and (2) compare the results with what has been reported in the literature. A finding that the COV_{ISRS} is comparable to or greater than what has been reported would further affirm that the current practice of using four or five input time histories may not be sufficient to attain stable ISRS estimates.

This paper uses the same statistical reasoning as PVP2020-21132 [3]. This approach is to use a relatively large number of input acceleration time histories to establish a relatively accurate estimate of the COV of the “true” mean ISRS, which is then used to determine whether a smaller number of acceleration time histories (e.g., four or five) can lead to a mean estimate of ISRS within $\pm 10\%$ of the “true” mean ISRS. Previous studies [6, 7] provided support that ISRS are more suitable for determining an adequate number of input time histories than the RS-matching criteria, because ISRS can represent the entire frequency range of interest for the structural responses, while the RS-matching criteria can only represent the maximum responses (i.e., the zero-period accelerations (ZPA) on the ISRS curves).

We emphasize that RS-matching methods may introduce some systematic characteristics or biases to the resultant time histories, which are extremely difficult to determine without a comprehensive comparison of many RS-matching algorithms. However, the conclusions in this paper are not expected to be affected by the chosen method because the focus of this work is on the uncertainties in ISRS, not on the systematic biases that individual RS-matching methods may introduce.

In this paper, we demonstrate how the seed time histories are modified using the new RS-matching algorithm, summarize the assumptions and the statistical procedure that were also used in PVP2020-21132, assess COV_{ISRS} based on RS-matched time histories, and compare them with the PSD-based time histories that consider only the uncertainties in the Fourier phase spectra. These results are also used to determine the number of time histories required to achieve stable estimates of ISRS. Since the amount of effort for RS matching is relatively large, we considered only one target RS (TRS), which is the Western U.S. RS shape for bin M7+D50-100, using the mid-bin properties $M = 7.5$ and $D = 75$ kilometers (km), as described in appendix B to SRP section 3.7.1 [1]. M and D stand for earthquake magnitude and source-to-site distance, respectively.

GENERATION OF RS-MATCHED INPUT TIME HISTORIES

This work required many RS-matched time histories; therefore, we developed a new program based on Reference [5] to automatically perform RS matching using parallel processing. This new program uses the same wavelet form as in Reference [5] and the same overall scheme to add wavelets at the times when the maximum responses occur in the RS calculation. However, our algorithm adds wavelets in a greedy fashion; each iteration adds only one wavelet at the frequency at which the calculated RS and the TRS differ the most among

all frequencies used for RS calculation. The algorithm in Reference [5] adds wavelets simultaneously at all frequencies in each iteration, weighted using a response matrix that has a size of the number of frequencies for RS matching. Therefore, the approach in this paper does not need to assemble and invert the response matrix to compute the weights. The new algorithm also includes some other differences to ensure efficiency and stability. Since the algorithm is not the focus of this paper, its details will be introduced in a different publication.

Using the selected TRS (Western U.S. RS with $M=7.5$, $D=75$ km [1]), we downloaded from the PEER NGA-West2 database [8] 291 seed acceleration time histories that have the highest similarity between their RS and the TRS. We also used the 1,902 seed time histories in the database associated with NUREG/CR-6728, “Technical Basis for Revision of Regulatory Guidance on Design Ground Motions: Hazard- and Risk-Consistent Ground Motion Spectra Guidelines,” issued October 2001 [9], without assessing their similarity to the TRS. This was necessary because we needed many seeds to reach a reasonable number of converged acceleration time histories to develop reliable ISRS statistics.

All seed time histories were set to match the TRS at 301 frequency points from 0.1 hertz (Hz) to 100 Hz, using a $\pm 5\%$ criterion that is the same as used in Reference [5]. It should be noted that this criterion is much tighter than the $[-10\%, 30\%]$ range used for design purposes [1, 2]. Each seed was matched with an initial limit of 2,000 wavelets. If an acceleration time history was not converged to the $\pm 5\%$ criterion, Gaussian noises with standard deviations at 5% of instantaneous absolute values of the time history were added, and the algorithm was rerun for another maximum of 2,000 wavelets. From the 2,193 seeds, we obtained 1,474 converged acceleration time histories.

One side effect of the wavelet-based time domain methods is that some low-frequency wavelets may be added before the start of some seed time histories. To maintain the same duration as the original seeds, the beginning parts of these added low-frequency wavelets were removed from the resultant time histories. Removing parts of these wavelets made many converged time histories violate the $\pm 5\%$ criterion in the RS comparison. Figure 1 shows that after the resultant time histories were chopped to maintain the same duration as the seeds, their comparison to the TRA deteriorated. The corresponding COV_{RS} , shown as the thin black curve, increased to about 22% at 0.1 Hz, compared to about 2% at higher frequencies where the agreement between the RS and the TRS is excellent. The COV_{RS} curve decreases from 22% to around 2% at 2 Hz and stays at that level for all higher frequencies. In this figure, the thin gray curves and the thick red curve represent the individual RS and the mean RS (M_{RS}), respectively, while the green and blue curves represent $M_{RS} \times (1 \pm COV_{RS})$. The curve for TRS is under the mean curve, not quite visible. Note that this figure was developed in the early stage of this work and did not use the final 1,474 converged time histories.

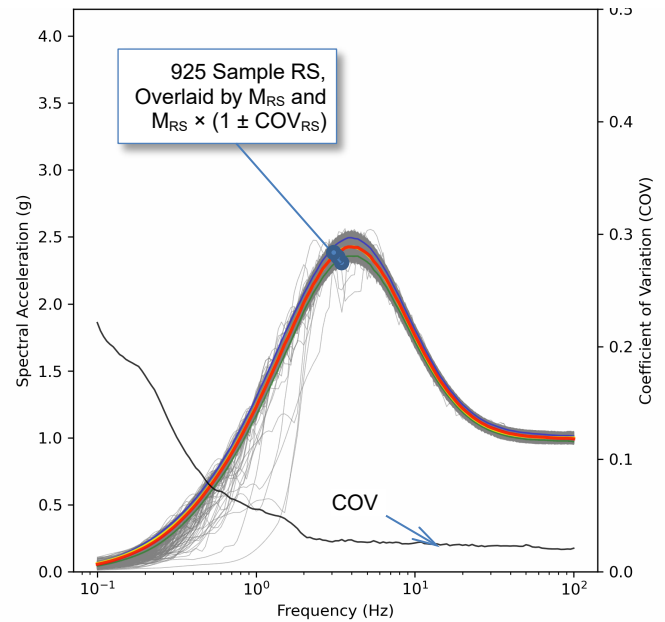


FIGURE 1: DEMONSTRATION OF THE EFFECT OF DETERIORATED RS COMPARISON AFTER CHOPPING THE RESULTANT TIME HISTORIES TO MAINTAIN THE SEED DURATION

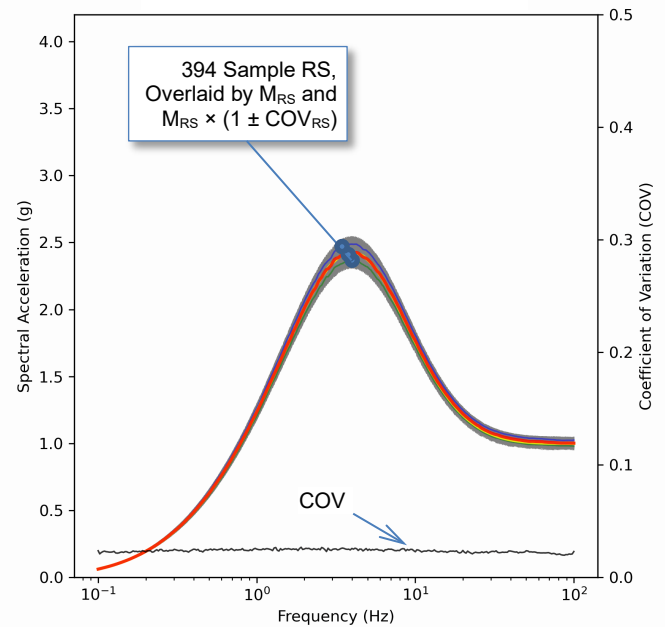


FIGURE 2: COMPARISON OF 394 SCREENED-IN TIME HISTORIES WITH THE TRS AND THE RESULTANT NEARLY CONSTANT, SMALL COV_{RS} AROUND 2%

There are ways to avoid adding wavelets before the start of the seeds, but the current implementation of our program achieves that manually through a graphical user interface. Therefore, instead of improving the algorithm to automatically achieve that goal, we screened the 1,474 converged time histories using the same $\pm 5\%$ criterion and obtained 394 final

time histories, which were then used in this study. Using the same colors and line styles as in figure 1, figure 2 compares the RS of the 394 screened-in time histories to the TRS and also shows the nearly constant, small COV_{RS} that is between 2% to 2.7% across the entire frequency range considered. The number of screened-in time histories is smaller than 500, which was used in PVP2020-21132; however, we think it can still yield relatively accurate estimate of sample COV_{ISRS} .

RECAP OF THE BASIC ASSUMPTIONS AND THE STATISTICAL PROCEDURE IN PVP2020-21132

Because input acceleration time histories are often generated using the same procedure or software and meet the same acceptance criteria for RS matching, they generally share some common features and may include systematic biases. However, the resultant time histories and their RS can be assumed to be statistically independent relative to their common features and biases. Further, the response time histories and the ISRS for the single-degree-of-freedom structures can also be assumed to be statistically independent. For simplicity, we also assume that ISRS have an identical distribution on a frequency-by-frequency basis. These assumptions are considered reasonable because the seeds used to generate these time histories are generally uncorrelated.

With these assumptions, we can use the sample COV to derive the COV for mean quantities. Using a large number (N) of RS-matched acceleration time histories to estimate an accurate sample COV of the input RS and the ISRS (COV_{RS} and COV_{ISRS} , respectively), the COV of the M_{RS} and the COV of the mean ISRS (M_{ISRS}), $COV_{M_{RS}}$ and $COV_{M_{ISRS}}$ can then be obtained as shown in equation (1):

$$\begin{aligned} COV_{M_{RS}} &= \frac{COV_{RS}}{\sqrt{N}} \\ COV_{M_{ISRS}} &= \frac{COV_{ISRS}}{\sqrt{N}} \end{aligned} \quad (1)$$

These quantities are functions of frequency, which is omitted from the symbols herein for simplicity. In this paper, we continue to use COV_{ISRS} to determine, for a selected confidence level (CL), how many input time histories are required to achieve a $\pm 10\%$ confidence interval within which the “true” M_{ISRS} falls. For two typical levels of CL, the smaller number (N_s) of samples to establish $\pm 10\%$ confidence interval can be calculated as shown in equation (2):

$$\begin{aligned} N_s &\geq 100 COV_{ISRS}^2, CL=68\% \\ N_s &\geq 384 COV_{ISRS}^2, CL=95\% \end{aligned} \quad (2)$$

These equations indicate that the required number of input acceleration time histories is a quadratic function of the sample CV_{ISRS} . Figure 3 shows that N_s increases faster than exponentially as a function of CL. Adopted from PVP2020-

21132 [3], table 1 lists the N_s calculated using equation (2) for some assumed sample CV_{ISRS} . Equation (2) and table 1 can be used to determine N_s if the sample COV_{ISRS} is known or accurately estimated.

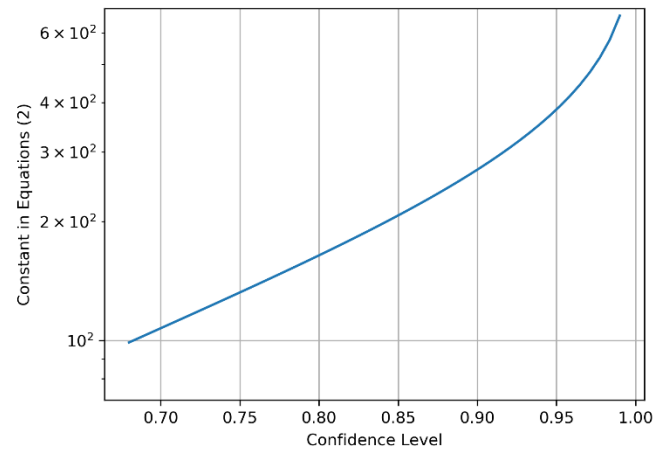


FIGURE 3: THE REQUIRED NUMBER OF TIME HISTORIES INCREASES AS A FUNCTION OF CONFIDENCE LEVEL FASTER THAN EXPONENTIALLY

TABLE 1: THE NUMBER OF INPUT TIME HISTORIES REQUIRED FOR A GIVEN SAMPLE COV_{ISRS} TO ACHIEVE A $\pm 10\%$ CONFIDENCE INTERVAL FOR THE MEAN ISRS

COV_{ISRS} (%)	N_s (CL = 68%)	N_s (CL = 95%)
20	4	15
22	5	19
26	7	26
30	9	35
40	16	61
50	25	96
70	49	188

SOURCE: Adapted from table 1 of PVP2020-21132 [3].

UNCERTAINTIES IN INPUT RS FOR RS-MATCHED INPUT TIME HISTORIES AND THOSE FOR PSD-BASED TIME HISTORIES

Figure 2 shows the RS of the 394 RS-matched input time histories, indicating an excellent agreement with the TRS as expected due to the tight RS-matching criteria. This figure also shows the COV_{RS} is between 2% and 2.7%, which is about half of the 5% RS-matching criterion. Given this level of COV, the 394 input time histories are judged to be reasonable for producing a good estimate of the sample COV_{ISRS} .

As a comparison, figure 4 shows the results using the 500 PSD-based time histories that were used for PVP2020-21132. This figure uses the same colors and line styles as in figure 1. The average RS of these time histories closely matched the same TRS, and the TRS curve is not visible because it is overlaid by the average RS. The Fourier amplitude spectra of these PSD-based time histories are the same, but their Fourier phase spectra were random. The COV_{RS} was found to be between 10% and 29%, significantly larger than the COV_{RS} for the RS-matched time histories by a factor of 11 for the maximum values. The COV_{RS} also generally decreases as a function of frequency, unlike the COV_{RS} for the RS-matched time histories that stays nearly at a constant value across the entire frequency range.

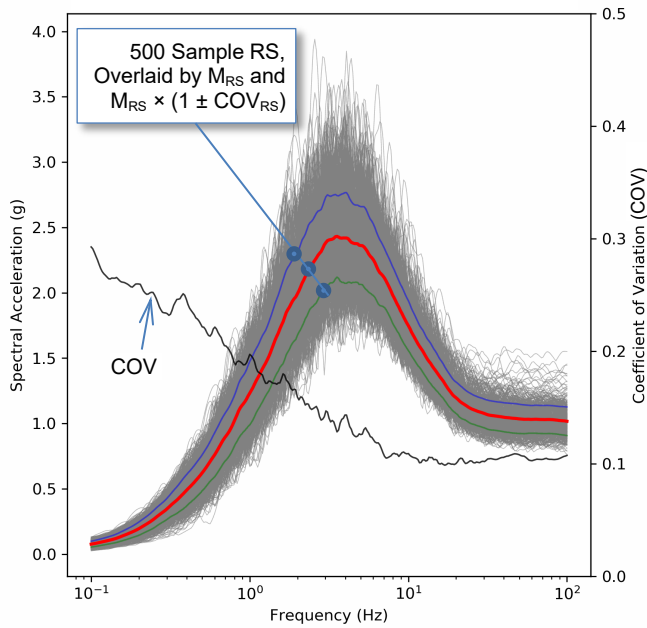


FIGURE 4: RS AND COV_{RS} OF THE 500 PSD-BASED INPUT MOTIONS GENERATED FOR WESTERN U.S. RS FOR BIN M7+D50-100

ASSESSMENT OF COV_{ISRS}

The significant differences in COV_{RS} between (1) the case of RS-matched time histories that include both amplitude and phase uncertainties and (2) the case of PSD-based time histories that include only phase uncertainties do not translate to COV_{ISRS} , as demonstrated in this section.

We used the same approach as in PVP2020-21132 to generate the ISRS for this work. As a summary, for each input time history, 151 single-degree-of-freedom oscillators with a damping ratio of 5% were used to generate response time histories. These oscillators cover a frequency range of 0.1 Hz to 100 Hz and can represent various modes of complex structures. The response time histories of an oscillator were generated in the frequency domain through the convolution of the oscillator’s transfer function and the Fourier spectra of the 394

RS-matched time histories. For each oscillator (conceptually, a single-degree-of-freedom structure or a structural mode), the RS of the 394 response time histories (i.e., the ISRS) were used to estimate the sample COV_{ISRS} for this oscillator.

Representative oscillators selected from the 151 oscillators are discussed below, with a focus on how they respond very differently to the RS-matched time histories and to the PSD-based time histories.

Oscillator at 0.49 Hz

The top plot in figure 5 shows the ISRS of a 0.49-Hz oscillator using 394 RS-matched time histories. The thin gray curves, the thick red curve, and the red dashed curves represent the individual ISRS, their mean M_{ISRS} , and $M_{ISRS} \times (1 \pm COV_{ISRS})$, respectively. The bottom plot shows the frequency-dependent COV_{ISRS} in blue, the COV_{RS} in red (also shown in figure 2), and their ratio as the gray dashed line. Figure 6 shows similar plots for the same oscillator subjected to the 500 PSD-based input time histories, which were part of the work for PVP2020-21132 [3].

Comparing these two figures, the COV_{ISRS} for the RS-matched time histories has been significantly “amplified” from the COV_{RS} of the input motions at the oscillator frequency by a factor greater than 8, while that factor is only about 1.3 for the PSD-based time histories. Although COV_{RS} for the RS-matched time histories is much smaller than COV_{RS} for the PSD-based time histories, the resultant COV_{ISRS} for the former is only slightly lower than that for the latter, 21% versus 30%.

The ZPA effect as reported in PVP2020-21132 for the PSD-based input time histories does not occur for the RS-matched time histories. The ZPA effect refers to an observation that COV_{ISRS} maintains the value of COV_{RS} at the oscillator frequency at frequencies higher than the ZPA frequency, after which the spectral acceleration equals ZPA. For example, as shown in figure 6, the COV_{ISRS} at frequencies higher than 4 Hz stays flat at the value of COV_{RS} at the oscillator frequency of 0.49 Hz.

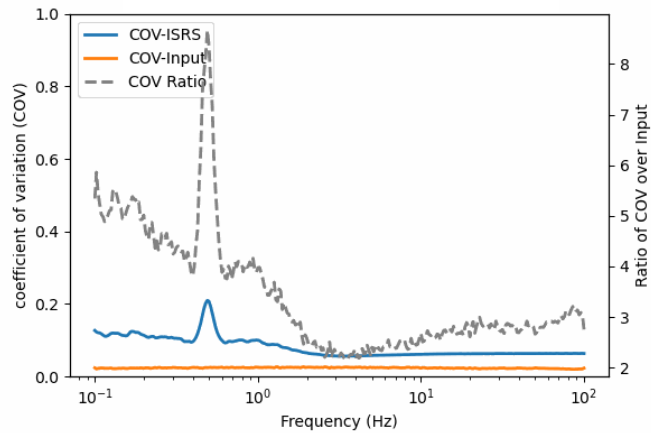
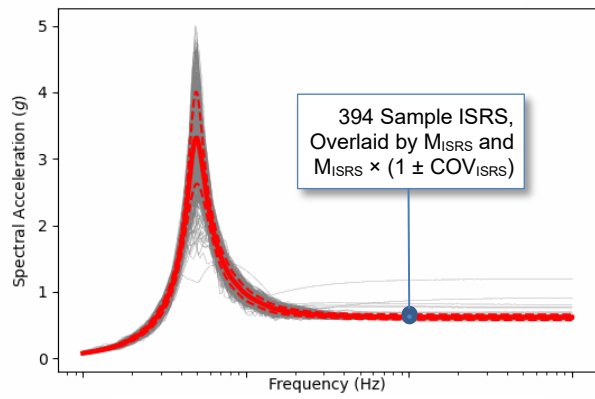


FIGURE 5: ISRS AND COV_{ISRS} FOR A 0.49-HZ OSCILLATOR USING 394 RS-MATCHED TIME HISTORIES

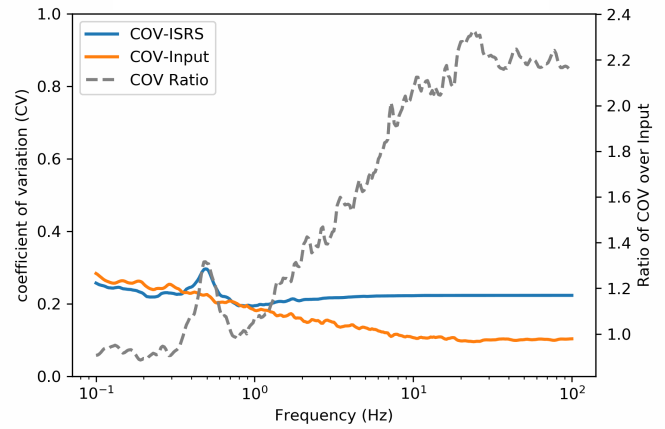
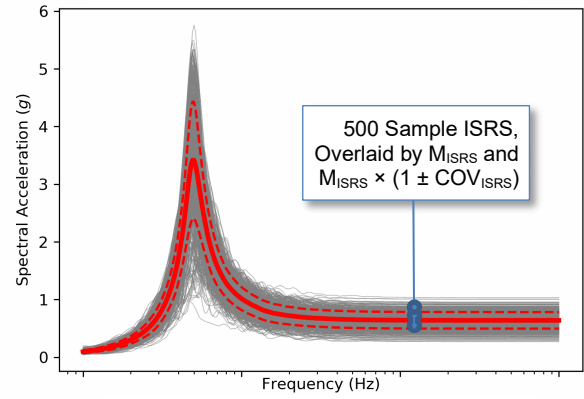


FIGURE 6: ISRS AND COV_{ISRS} FOR A 0.49-HZ OSCILLATOR USING 500 PSD-BASED TIME HISTORIES

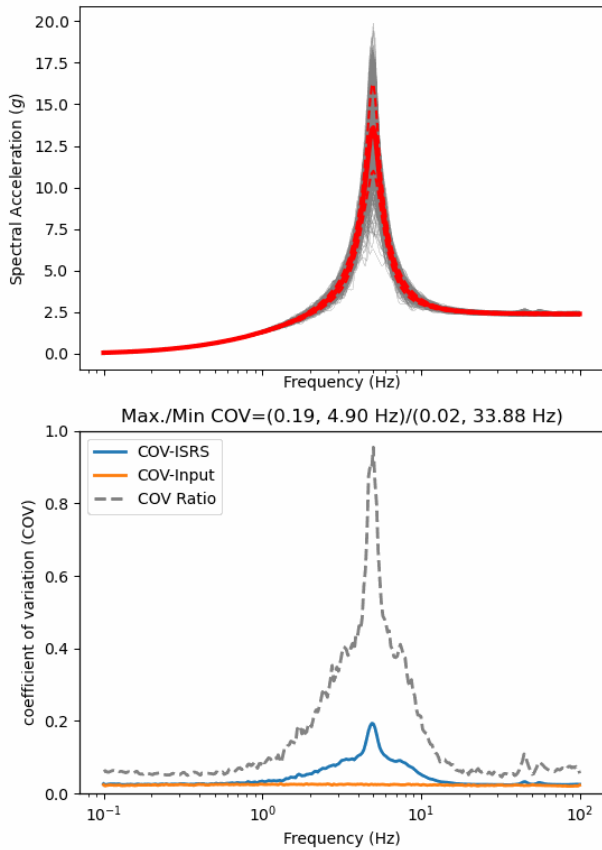


FIGURE 7: ISRS AND COV_{ISRS} FOR A 4.97-HZ OSCILLATOR USING 394 RS-MATCHED TIME HISTORIES

Oscillator at 4.97 Hz

Figure 7 and figure 8 show similar plots for another oscillator with a frequency of 4.97 Hz for the RS-matched time histories and for the PSD-based time histories, respectively. Similar to the 0.49-Hz oscillator, this oscillator significantly “amplified” the COV at the oscillator frequency for the RS-matched time histories. Although the COV_{RS} for the RS-matched time histories is much smaller, the corresponding COV_{ISRS} becomes larger than that for the PSD-based time histories at the oscillator frequency.

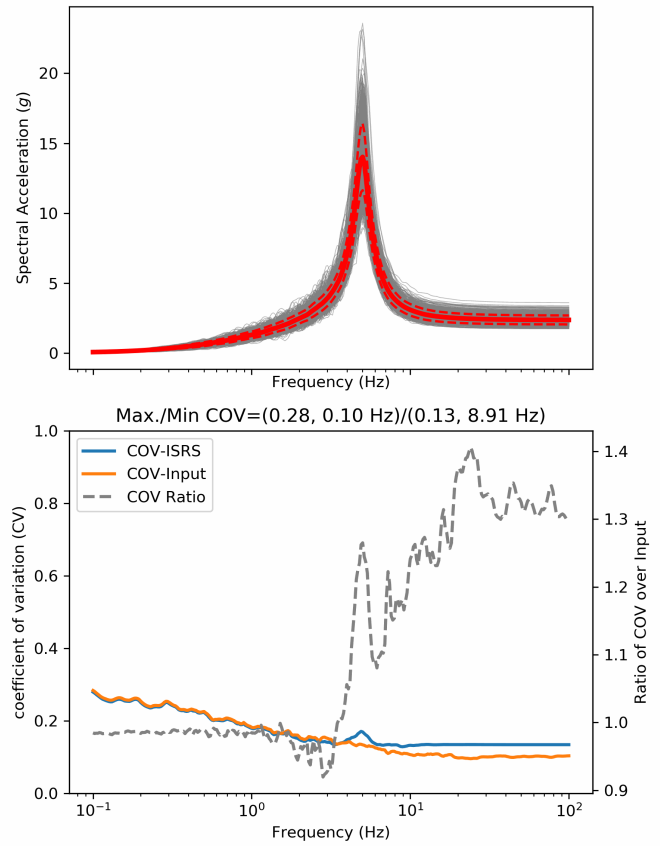


FIGURE 8: ISRS AND COV_{ISRS} FOR A 4.97-HZ OSCILLATOR USING 500 PSD-BASED TIME HISTORIES

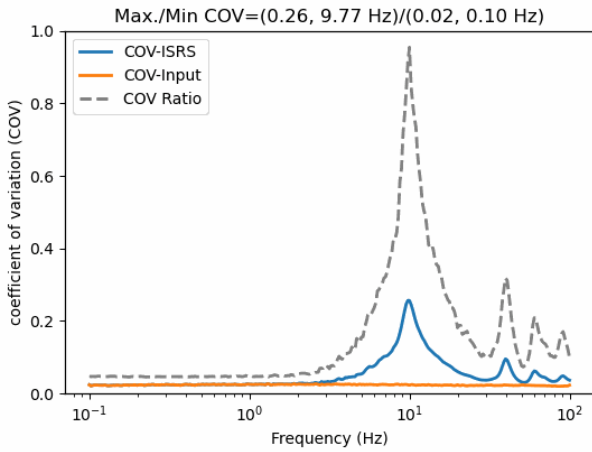
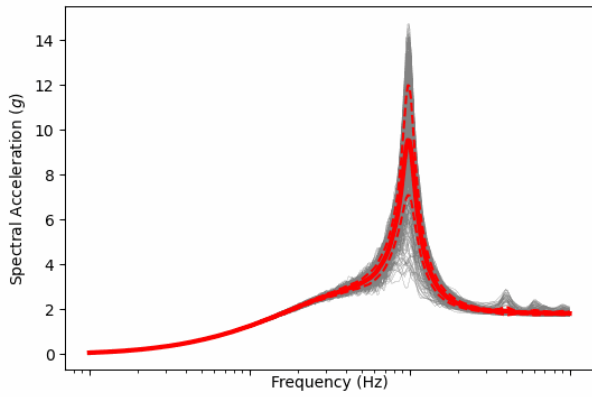


FIGURE 9: ISRS AND COV_{ISRS} FOR A 9.89-HZ OSCILLATOR USING 394 RS-MATCHED TIME HISTORIES

Oscillator at 9.89 Hz

Figure 9 and figure 10 show an oscillator with a frequency of 9.89 Hz for the RS-matched time histories and for the PSD-based time histories, respectively. Compared to the previous two oscillators, this oscillator “amplified” the COV even more for the RS-matched time histories by a factor of more than 11. It barely amplified the COV for the PSD-based time histories. Although the COV_{RS} for the RS-matched time histories is still much smaller by a factor of 5 at the oscillator frequency, the corresponding COV_{ISRS} approximately doubles that for the PSD-based time histories.

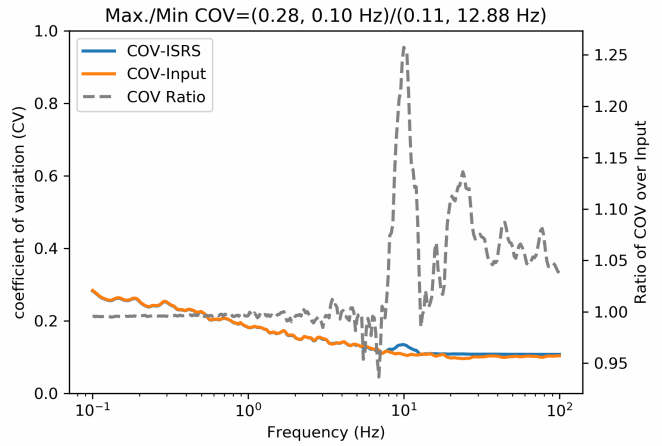
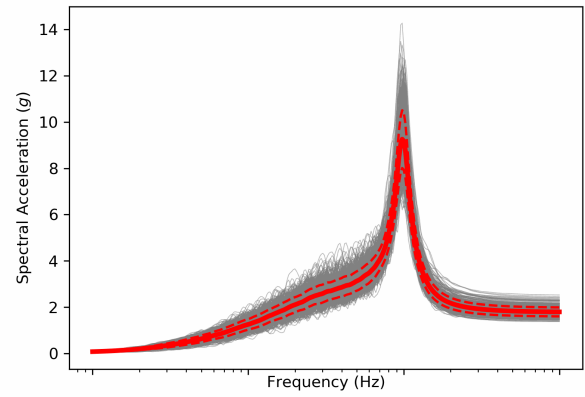


FIGURE 10: ISRS AND COV_{ISRS} FOR A 9.89-HZ OSCILLATOR USING 500 PSD-BASED TIME HISTORIES

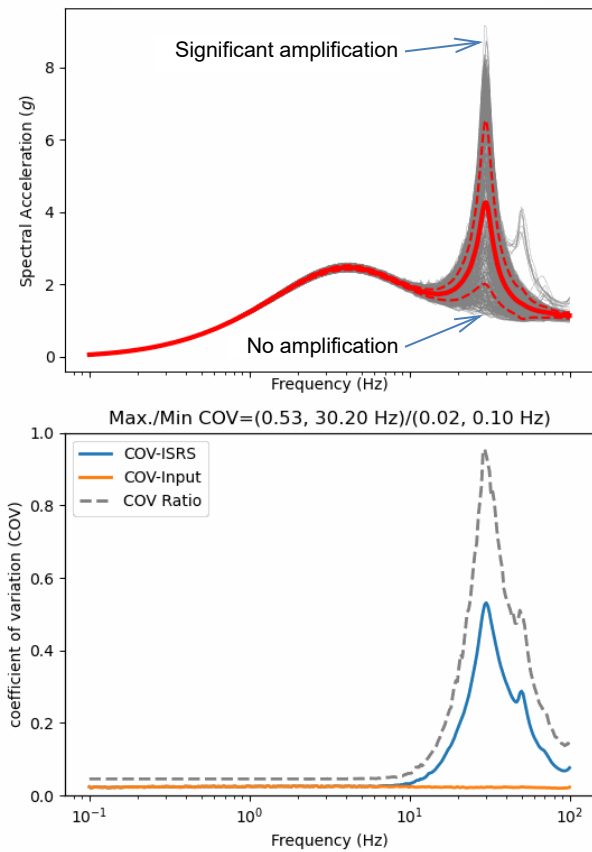


FIGURE 11: ISRS AND COV_{ISRS} FOR A 29.99-HZ OSCILLATOR USING 394 RS-MATCHED TIME HISTORIES

Oscillator at 29.99 Hz

Figure 11 and figure 12 show the results for the 29.99-Hz oscillator for the RS-matched time histories and PSD-based time histories, respectively. Compared to the previous cases, this oscillator significantly “amplified” the COV for the RS-matched time histories by a factor of 27. In contrast, there is essentially no amplification of the COV for the PSD-based time histories. The COV_{RS} for the RS-matched time histories is still one-fifth of that for the PSD-based time histories at the oscillator frequency, but the corresponding COV_{ISRS} is about 5 times that for the PSD-based time histories.

It is interesting to note that for the RS-matched time histories, the ISRS of some input time histories do not show any amplification, while others show significant amplification at the oscillator frequency. As a comparison, the ISRS for the PSD-based time histories have relatively more consistent amplification at the same oscillator frequency than the RS-matched time histories.

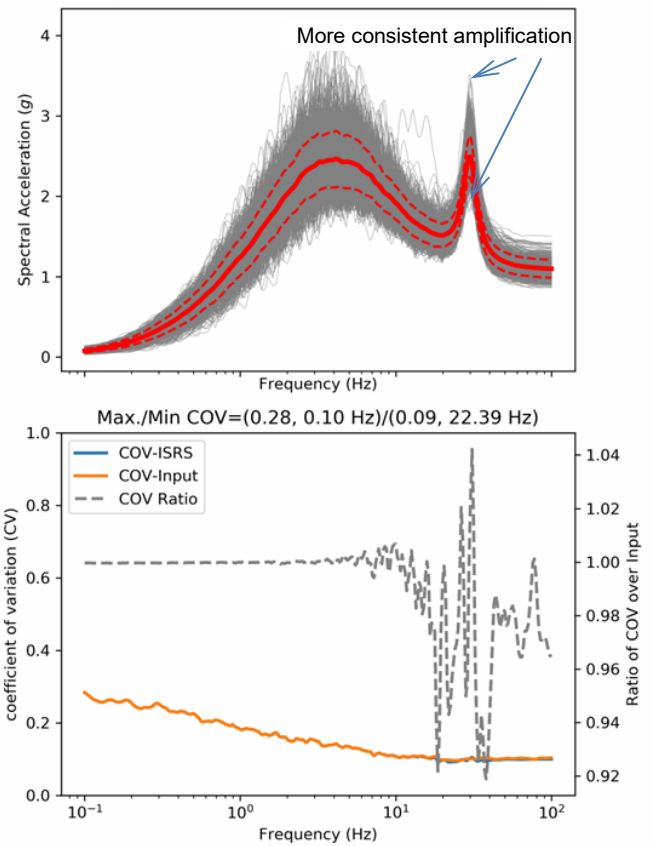


FIGURE 12: ISRS AND COV_{ISRS} FOR A 29.99-HZ OSCILLATOR USING 500 PSD-BASED TIME HISTORIES

Overall Assessment of the 151 Oscillators

Figure 13 and figure 14 summarize the COV_{ISRS} for all 151 oscillators for the RS-matched time histories and the PSD-based time histories respectively. There are many different curves for individual COV_{ISRS} and related statistics, but our focus is on the two thick, yellow curves that envelop the COV_{ISRS} values at the oscillator frequencies, representing how the COV_{RS} gets “amplified.” These two curves represent how the two types of input time histories can result in COV_{ISRS} for structural modes in the frequency range from 0.1 Hz to 100 Hz.

For the RS-matched time histories, the COV_{ISRS} is around 20%, relatively flat between 0.2 Hz and 6 Hz. For a frequency reference, the spectral peak for the TRS is around 4 Hz. After 6 Hz, the COV_{ISRS} increases quickly, to 40% at 18 Hz, and to around 68% at 60 Hz. COV_{ISRS} appears to be independent of COV_{RS} , which is nearly a constant value of 2% across the entire frequency range. COV_{ISRS} being independent of COV_{RS} reveals that the variation in ISRS is not caused by the variation of the input RS for the RS-matched time histories. We believe COV_{ISRS} is actually caused by the PSD variation of the input motions. This is the reason why we have enclosed in quotation marks all terms related to “amplification.” Reference [6] has shown that (1) ISRS reflect the power distribution of the input motion, and (2) RS is an inadequate descriptor of the input

motion without particular consideration of PSD. For the RS-matched time histories using the newly developed, greedy, wavelet-based RS-matching algorithm, the relatively flat COV_{ISRS} from 0.2 Hz to 6 Hz largely indicates that the power in this frequency range varies less than other frequency ranges, while the large COV_{ISRS} increase above 6 Hz indicates the PSD variation increases greatly. We reiterate that the variation of COV_{ISRS} also depends on the method used to generate the RS-matched time histories.

For the PSD-based time histories, the COV_{ISRS} gradually decreases from 38% to about 8% from 0.1 Hz to 100 Hz. Compared to the COV_{RS} shown in figure 4, the COV_{ISRS} has small increases at lower frequencies and gradually approaches the COV_{RS} at higher frequencies. As shown in PVP2020-21132 [3], COV_{RS} decreases monotonically from 30% to about 7% for the PSD-based time histories, regardless of the TRS shape. This is a great advantage for the PSD-based time histories, because (1) their COV_{ISRS} is smaller than those for the RS-matched time histories, (2) their COV_{ISRS} is well defined as monotonically decreasing functions of frequency, and (3) the PSD-based time histories contain only uncertainties in Fourier phase spectra, which are considered irreducible.

Overall, even though the RS-matched time histories have a maximum COV_{RS} that is only one-eleventh of that for the PSD-based time histories, their corresponding COV_{ISRS} is generally and significantly larger than the latter for frequencies above 2 Hz. For ISRS below 2 Hz, although the shapes of COV_{ISRS} are somewhat different between these two cases (as shown in figure 13 and figure 14), they represent a similar COV level and similar trend. The screening procedure in this study, which affects mainly low-frequency wavelets, might have made the COV_{ISRS} for the RS-matched time histories somewhat smaller than that for the PSD-based time histories.

SUMMARY

The maximum COV_{ISRS} was found to be 68% for the RS-matched time histories, generally confirming the 70% value reported in PVP2010-25919 [4]. A few differences exist between that study and this one. A frequency domain RS-matching method was used for PVP2010-25919 [4]. The 70% COV_{ISRS} value occurred at 10.5 Hz in that study. At that frequency, the COV_{ISRS} was only 28% in this study. Note that PVP2010-25919 [4] used real structures and soil structure interaction analyses, while this study considered only single-degree-of-freedom systems. Modal combinations are likely to increase COV_{ISRS} , at least for frequency ranges where the COV_{ISRS} is lower than its neighboring frequency ranges.

To achieve a stable mean estimate of ISRS that is within $\pm 10\%$ of the “true” mean, using equation (2) or table 1, a maximum COV_{ISRS} of 70% suggests that the required number of input time histories is 49 for a confidence level of 68%, and 188 for a confidence level of 95%. These high numbers of input time histories would not be practical in most applications.

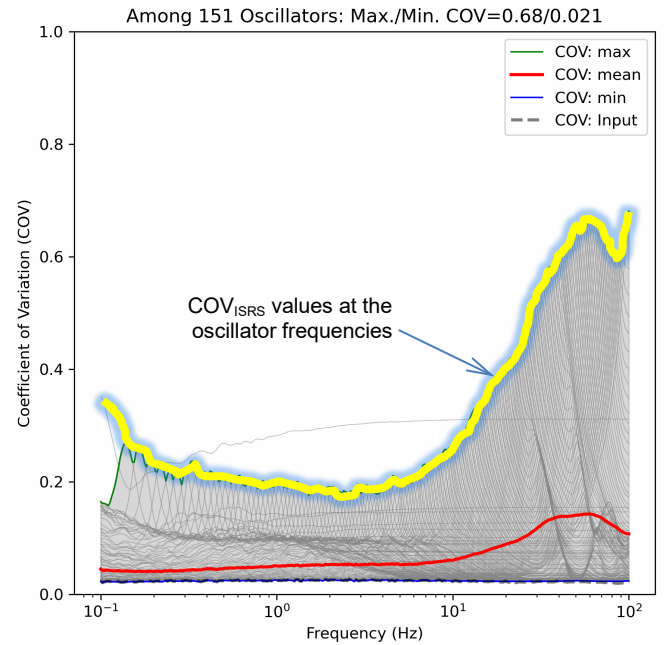


FIGURE 13: COV_{ISRS} FOR 151 OSCILLATORS USING 394 RS-MATCHED TIME HISTORIES

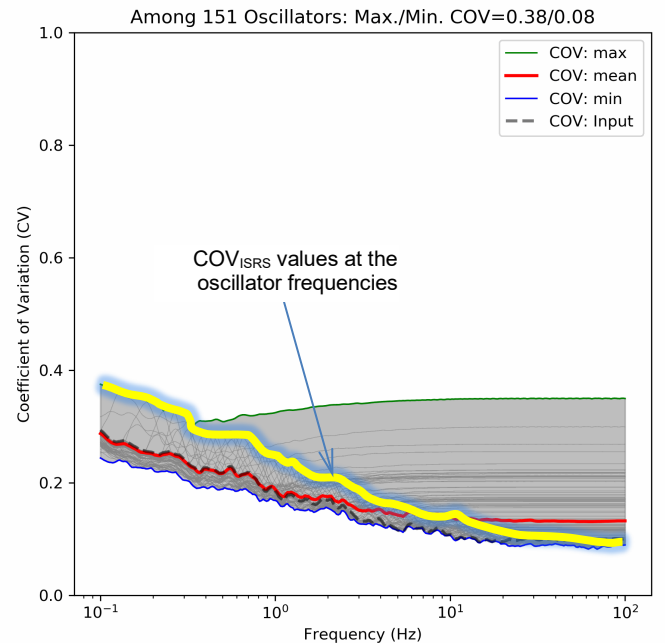


FIGURE 14: COV_{ISRS} FOR 151 OSCILLATORS USING 500 PSD-BASED TIME HISTORIES

This work confirms the conclusion in PVP2020-21132 [3] that the current practice of using four or five input time histories should be conditioned by explicitly checking their PSD functions for sufficient power contents in the frequency range of interest to the responses. In addition, we have provided further evidence using RS-matched time histories to support that a check of PSD functions is necessary even using multiple input time histories, because their mean ISRS estimate,

although not as stable as necessarily required for reasonable levels of confidence, would tend to vary on the conservative side.

It should be noted that Section 3.7.1, “Seismic Design Parameters,” of NUREG-0800 [1] already indicates the necessity of a PSD check in Option 2, “Multiple Sets of Time Histories.” This study and PVP2020-21132 provide the quantitative reasoning for this necessity. The results in this study, PVP2010-25919, and PVP2020-21132 can also serve as the necessary technical bases for consistent technical positions between the ASCE/SEI 4-16 [2] and NUREG-0800 [1]. The current RS convergence criteria in ASCE/SEI 4-16 practically do not require a PSD check.

REFERENCES

1. U.S. Nuclear Regulatory Commission, “Standard Review Plan for the Review of Safety Analysis Reports for Nuclear Power Plants: LWR Edition,” NUREG-0800, Washington, DC.
2. American Society of Civil Engineers (ASCE)/Structural Engineering Institute (SEI) 4-16, “Seismic Analysis of Safety-Related Nuclear Structures,” Reston, Virginia.
3. Nie, J.R., J. Xu, V. Graizer, and D. Seber (2020). “Estimating stable mean responses for linear structural systems by using a limited number of acceleration time histories,” *American Society of Mechanical Engineers Pressure Vessels and Piping Conference* (PVP2020-21132), Minnesota (virtual).
4. Houston, T.W., G.E. Mertz, M.C. Costantino, and C.J. Costantino (2010). “Investigation of the impact of seed record selection on structural response,” *American Society of Mechanical Engineers Pressure Vessels and Piping Conference* (PVP2010-25919), Bellevue, Washington.
5. Atik, L., and N. Abrahamson (2010). “An improved method for nonstationary spectral matching,” *Earthquake Spectra*, 26(3), 601–617.
6. Nie, J.R., J. Pires, and D. Seber (2019). “Understanding the assumptions in design response spectra for seismic time history analyses,” *Transactions*, SMiRT-25, Charlotte, North Carolina.
7. U.S. Nuclear Regulatory Commission, Research Information Letter RIL-2019-01 (2019). “Assessment of Artificial Acceleration Time History Guidance in Standard Review Plan Section 3.7.1, ‘Seismic Design Parameters,’” Washington, DC. Agencywide Documents Access and Management System Accession No. ML19308A045.
8. PEER NGA-West2 database: <https://ngawest2.berkeley.edu/>.
9. NUREG/CR-6728, “Technical Basis for Revision of Regulatory Guidance on Design Ground Motions: Hazard- and Risk-consistent Ground Motion Spectra Guidelines,” issued October 2001, Washington, DC.